

1  
2  
3  
4 **New solution method to produce high performance thermoelectric ceramics:**  
5  
6 **a case study of Bi-Sr-Co-O**

7  
8  
9 M. A. Madre, Sh. Rasekh, J. C. Diez, A. Sotelo\*

10  
11 ICMA (CSIC-Universidad de Zaragoza), M<sup>a</sup> de Luna, 3. 50018 Zaragoza, Spain.  
12  
13  
14

15  
16 **Abstract**  
17

18  
19 Bi<sub>2</sub>Sr<sub>2</sub>Co<sub>1.8</sub>O<sub>x</sub> ceramics have been synthesized through a solution method involving  
20  
21 the addition of polyethyleneimine as coordinating agent for the metallic cations.  
22  
23 From these powders, bulk sintered materials have been prepared. Microstructure  
24  
25 has been studied by means of scanning electronic microscopy (SEM) and it has  
26  
27 shown that samples are mainly composed by the thermoelectric phase, with very  
28  
29 small amounts of secondary phases. Electrical resistivity measurements showed  
30  
31 very small values (around 21mΩ.cm at room temperature), nearly constant with  
32  
33 temperature, while thermopower increases rapidly to values higher than 200μV/K  
34  
35 at 650°C. Power factor value at 50°C is about 0.08mW/K<sup>2</sup>.m and 0.20 at 650°C,  
36  
37 which makes this ceramic a potential material for power generation applications.  
38  
39  
40  
41  
42  
43  
44

45  
46 Keywords: Synthesis, Ceramics, Thermopower, Electrical resistivity, Power factor.  
47  
48  
49

50  
51 Corresponding author: A. Sotelo. ICMA (CSIC-Universidad de Zaragoza), M<sup>a</sup> de  
52  
53 Luna, 3. 50018 Zaragoza, Spain. Tel.: +34 976762617. Fax: +34 976761957. e-  
54  
55 mail address: [asotelo@unizar.es](mailto:asotelo@unizar.es)  
56  
57  
58  
59  
60  
61  
62  
63  
64  
65

## 1. Introduction

From the discovery of ceramic oxides with high thermoelectrical properties [1], cobaltite ceramics have attracted attention due to their performances [2,3]. Many different conformation techniques have been used in order to obtain bulk thermoelectrical properties close to those obtained in single crystals, as reactive templated grain growth (RTGG) [4, 5], templated grain growth (TGG) [6], hot pressing (HP) [7], and spark plasma sintering [8]. Most of these processes use powders prepared by the classical solid state reaction method which is characterized by several mixing, milling and calcination processes. In spite of these repeated processes, typical materials show incomplete reaction and compositional inhomogeneities that influence their final properties. In this context, solution syntheses appear as a solution to improve the precursor homogeneity, together with smaller particle size, which result on the increase of the precursors reactivity. These changes on the precursors can help improving the thermoelectrical performances of those polycrystalline cobaltites which is of the main importance in order to be used in power generation devices reaching high thermal-to-electrical energy conversion.

In this contribution it is presented a solution method, used for the first time on the cobaltite materials, involving a polymer addition to produce high performance bulk thermoelectric Bi-Sr-Co-O ceramics.

## 2. Experimental

### 2.1. Precursors preparation

1  
2  
3  
4 Synthesis of Bi-Sr-Co-O precursors was made in several steps. Firstly, adequate  
5  
6 amounts of metallic acetates (analytical grade) were dissolved in a mixture of  
7  
8 glacial acetic acid and distilled water (~ 40:60vol.%, respectively).  
9

10  
11 Polyethyleneimine (PEI, 50wt.% water) was added (~ 1 mol PEI:2 moles  
12  
13  $\text{Bi}_2\text{Sr}_2\text{Co}_{1.8}\text{O}_x$ ) to the solution which turned darker immediately indicating the  
14  
15 cation-nitrogen coordination. Solvent evaporation was produced in a rotary  
16  
17 evaporator reducing the initial volume to about 20%. Total solvent evaporation is  
18  
19 performed on a hot plate at about 50°C until a dark pink thermoplastic paste is  
20  
21 obtained. Further heating turned this paste to violet color, followed by a partial  
22  
23 decomposition and, finally, producing a self propagated combustion at about 300-  
24  
25 350°C which raises immediately the temperature inside the crucible to about 750°C  
26  
27 measured with an IR optical pyrometer.  
28  
29  
30  
31  
32

33 The obtained powders were manually milled, thermally treated at 750 and 810°C  
34  
35 for 6 hours, with an intermediate milling, uniaxially pressed at 400MPa in form of  
36  
37 prisms (~ 3x3x14mm<sup>3</sup>) and then sintered at 870°C for 24 hours under air, with  
38  
39 furnace cooling.  
40  
41  
42

43 Sintered materials were characterized by powder X-ray diffraction (XRD, Rigaku  
44  
45 D/max-B). The platelet thickness was estimated from X-ray line broadening  
46  
47 measurements, the calculation was done using the (006) and (008) diffraction  
48  
49 peaks, according to the Scherrer formula [9]. Microstructural characterization was  
50  
51 performed by scanning electron microscopy (SEM, JEOL 6000) provided with an  
52  
53 energy dispersive spectroscopy (EDS) system. Micrographs of transversal  
54  
55 fractured and longitudinal polished sections of the samples have been recorded to  
56  
57  
58  
59  
60  
61  
62  
63  
64  
65

1  
2  
3  
4 analyze the grain sizes and shapes as well as the different phases and their  
5  
6 distribution.  
7  
8  
9

## 10 11 *2.2. Thermoelectrical characterization*

12  
13  
14 Electrical resistivity ( $\rho$ ) and thermopower ( $S$ ), were simultaneously determined by  
15  
16 the standard dc four-probe technique in a LSR-3 measurement system (Linseis  
17  
18 GMBh). They were measured in the steady state mode at temperatures ranging  
19  
20 from 50 to 650°C under He atmosphere. With the electrical resistivity and  
21  
22 thermopower data, the power factor ( $PF=S^2/\rho$ ) has been calculated in order to  
23  
24 determine the samples performances.  
25  
26  
27  
28  
29  
30

## 31 **3. Results and discussion**

32  
33  
34 Fig. 1 shows the XRD plot for the  $\text{Bi}_2\text{Sr}_2\text{Co}_{1.8}\text{O}_x$  samples. Most of the peaks  
35  
36 correspond to the thermoelectric phase, with minor peaks associated to non-  
37  
38 thermoelectrical secondary phases. The highest peaks (marked with a \*) belong to  
39  
40 the misfit cobaltite phase and are in agreement with previously reported data  
41  
42 [4,10]. The other peaks correspond to the minor  $\text{Bi}_{0.75}\text{Sr}_{0.25}\text{O}_y$  phase, with  
43  
44  $R\bar{3}m(\#166)$  space group (marked with a ●) [11] and to the Si (111) peak (indicated  
45  
46 by a #) used as reference. The XRD results indicate that nearly pure  $\text{Bi}_2\text{Sr}_2\text{Co}_{1.8}\text{O}_x$   
47  
48 phase was obtained in a relatively short sintering time.  
49  
50  
51  
52  
53  
54  
55  
56  
57  
58  
59  
60  
61  
62  
63  
64  
65

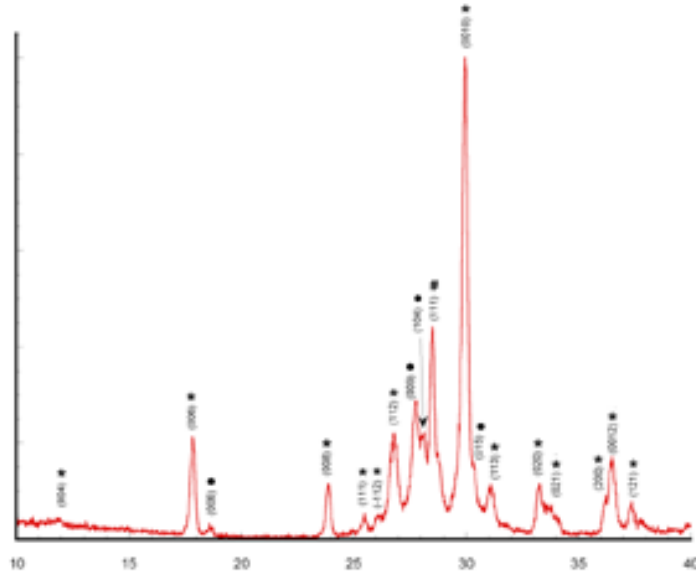


**Fig. 1.** XRD plot of the  $\text{Bi}_2\text{Sr}_2\text{Co}_{1.8}\text{O}_x$  samples. Peaks are marked with a \* for the thermoelectric  $\text{Bi}_2\text{Sr}_2\text{Co}_{1.8}\text{O}_x$  phase, •  $\text{Bi}_{0.75}\text{Sr}_{0.25}\text{O}_y$  non thermoelectric phase ( $R\bar{3}mH'$ ), and # for Si (used as reference).

Typical transversal fractured section of the sintered specimens is represented in Fig.2a. It is clear that samples are composed of randomly oriented plate-like grains, most of them exceeding  $10\mu\text{m}$  in the ab planes. On the other hand, thickness is difficult to be measured as they are, in turn, formed by many thin grains well stacked along the ab planes. In order to overcome this problem, the individual plate-like grain thickness has been estimated from the X-ray line broadening measurements using the (006) and (008) diffraction lines of the  $\text{Bi}_2\text{Sr}_2\text{Co}_{1.8}\text{O}_x$  phase, according to the Scherrer formula. The obtained mean value for the grain thickness is about  $35\text{nm}$  which clearly indicates that the crystal preferential growth is produced along the ab plain (coincident with the conduction CoO planes).

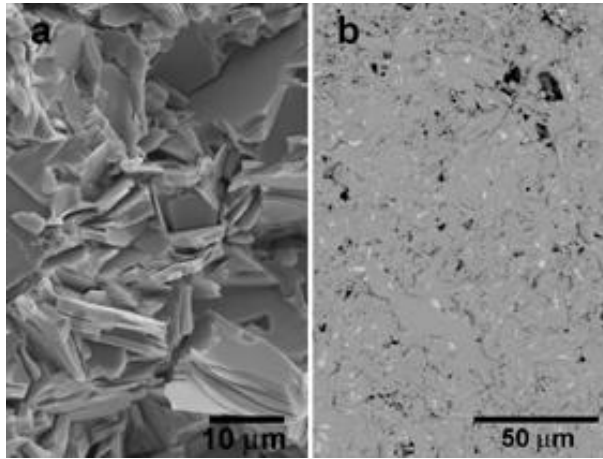
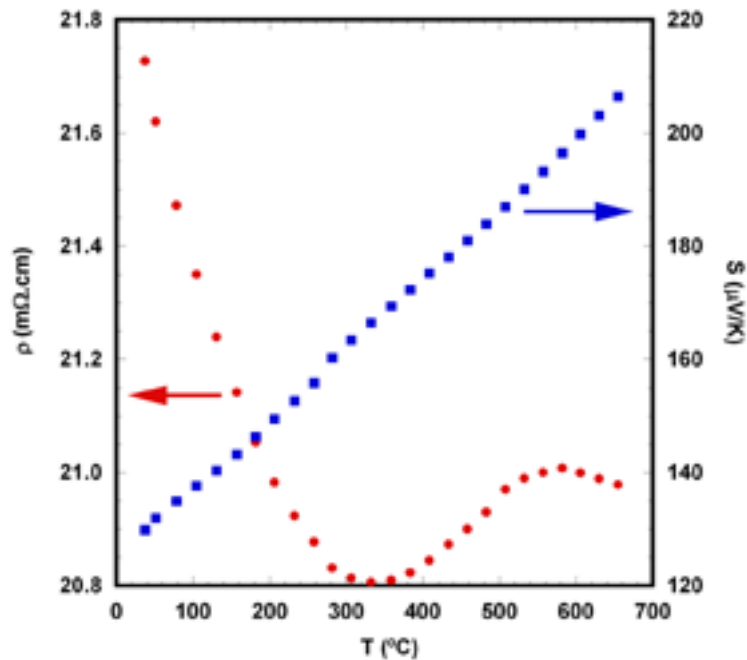


**Fig. 2.** Representative SEM micrographs of  $\text{Bi}_2\text{Sr}_2\text{Co}_{1.8}\text{O}_x$  ceramics. a) transversal fractured surface, and b) longitudinal polished surface. Different contrasts correspond to  $\text{Bi}_2\text{Sr}_2\text{Co}_{1.8}\text{O}_x$  (grey), SrO (dark grey), and  $\text{Bi}_{0.75}\text{Sr}_{0.22}\text{O}_y$  (white).

When observing the longitudinal polished section of  $\text{Bi}_2\text{Sr}_2\text{Co}_{1.8}\text{O}_x$  (Fig. 2b) it is found that major phase is the grey one with very small amounts of secondary phases (white and dark grey contrasts). EDS analysis performed on different points for each contrast showed that the grey one correspond to the thermoelectric  $\text{Bi}_2\text{Sr}_2\text{Co}_{1.8}\text{O}_x$  phase, dark grey to SrO, and white to  $\text{Bi}_{0.75}\text{Sr}_{0.22}\text{O}_y$  (very close to the  $\text{Bi}_{0.75}\text{Sr}_{0.25}\text{O}_y$  composition, determined by XRD). The amount of the different phases has been performed on several micrographs using Digital Micrograph software. The determined phase amounts have been around 5vol% for the  $\text{Bi}_{0.75}\text{Sr}_{0.22}\text{O}_y$  phase, 2vol.% SrO, and 93vol.% thermoelectric  $\text{Bi}_2\text{Sr}_2\text{Co}_{1.8}\text{O}_x$  phase. On the other hand, SrO phase found on the polished samples has not been found in the XRD due to its small proportion in the samples.

1  
2  
3  
4 The evaluation of the porosity has been performed using the apparent density of  
5  
6 the samples. In all cases, it has been shown to be  $91\pm 2\%$  of the theoretical  
7  
8 density.  
9

10  
11 The temperature dependence of the resistivity is shown in Fig. 3. As it can be  
12  
13 easily seen, the  $\rho(T)$  curve shows a very small variation with temperature, with a  
14  
15 semiconducting-like behaviour from room temperature to about  $350^\circ\text{C}$ , changing to  
16  
17 metallic-like behaviour from  $350$  to about  $600^\circ\text{C}$  and remaining practically constant  
18  
19 at higher temperatures. The very low resistivity values found in these samples are  
20  
21 due to the small content of secondary phases and porosity. As a consequence,  
22  
23 these values are close to the values obtained for textured materials ( $\sim 15\text{m}\Omega\cdot\text{cm}$  at  
24  
25  $275^\circ\text{C}$ ) [5] or single crystals ( $\sim 18\text{m}\Omega\cdot\text{cm}$  at room temperature) [4].  
26  
27  
28  
29  
30



31  
32  
33  
34  
35  
36  
37  
38  
39  
40  
41  
42  
43  
44  
45  
46  
47  
48  
49  
50  
51  
52  
53  
54  
55 **Fig. 3.** Temperature dependence of  $\rho$  (●) and S (■) for polycrystalline  $\text{Bi}_2\text{Sr}_2\text{Co}_{1.8}\text{O}_x$   
56  
57 materials.  
58  
59  
60  
61  
62  
63  
64  
65

1  
2  
3  
4 As it can be also seen in Fig. 3, where S vs. T is represented, the values are  
5  
6 positive in the entire temperature range, indicating a hole conduction mechanism.  
7  
8 On the other hand, they increase almost linearly with temperature, with values of  
9  
10 about  $130\mu\text{V}/\text{K}$  at  $\sim 50^\circ\text{C}$  which are higher than those obtained for textured  
11  
12 materials ( $125\mu\text{V}/\text{K}$  at  $275^\circ\text{C}$ ) [5] or single crystals ( $110\mu\text{V}/\text{K}$  at  $25^\circ\text{C}$ ) [4]. This high  
13  
14 value is due to the reduction of the cobalt oxidation state in the  $\text{CoO}_2$  layer,  
15  
16 calculated from Koshibae's relation [12]. These values are about 3.57 for the  
17  
18 measured samples (instead 3.63 for the stoichiometric ones [13]), clearly indicating  
19  
20 that the synthetic method generates higher amount of oxygen vacancies than the  
21  
22 usual methods.  
23  
24  
25  
26  
27

28  
29 In order to estimate the samples performances, PF values were calculated as a  
30  
31 function of temperature and represented in Fig. 4. Comparing the graphics from S  
32  
33 (Fig. 3) and PF (Fig. 4), they follow a parallel evolution with temperature due to the  
34  
35 small variations of  $\rho$  with temperature. At room temperature, the PF value of about  
36  
37  $0.075\text{mW}/\text{K}^2.\text{m}$  is higher than the obtained for single crystals ( $0.06\text{mW}/\text{K}^2.\text{m}$ ) [4]  
38  
39 and very close to textured materials ( $0.1\text{mW}/\text{K}^2.\text{m}$ ) [5].  
40  
41  
42  
43  
44  
45  
46  
47  
48  
49  
50  
51  
52  
53  
54  
55  
56  
57  
58  
59  
60  
61  
62  
63  
64  
65



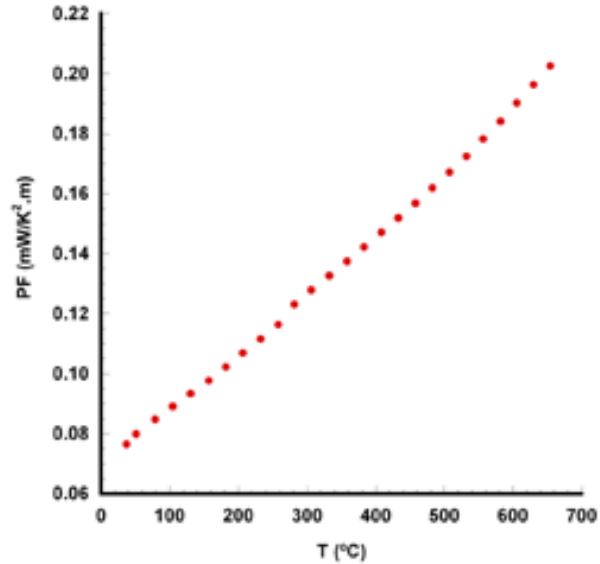


**Fig. 4.** Temperature dependence of PF for polycrystalline  $\text{Bi}_2\text{Sr}_2\text{Co}_{1.8}\text{O}_x$  materials.

#### 4. Conclusions

All the results indicate that the PEI method produces high quality and homogeneous polycrystalline ceramic materials with low amounts of secondary phases and porosity, leading to compacts with improved thermoelectrical properties comparable to those obtained for single crystals and textured materials.

#### 5. Acknowledgements

This research has been supported by the Spanish Ministry of Science and Innovation (Project MAT2008-00429). The authors wish to thank the Gobierno de Aragón (Project PI154/08 and Consolidated Research Groups T12 and T72) for financial support; also to C. Gallego, C. Estepa and J. A. Gomez for their technical assistance.

## 6. References

- [1] Terasaki I, Sasago Y, Uchinokura K. Phys. Rev. B 1997;56:12685.
- [2] Funahashi R, Matsubara I, Ikuta H, Takeuchi T, Mizutani U, Sodeoka S. Jpn. J. Appl. Phys. 2000;39:L1127.
- [3] Masset AC, Michel C, Maignan A, Hervieu M, Toulemonde O, Studer F, Raveau B, Hejtmanek J. Phys. Rev. B 2000;62:166.
- [4] Itoh T, Terasaki I. Jpn. J. Appl. Phys. 2000;39:6658.
- [5] Itahara H, Xia C, Sugiyama J, Tani T. J. Mater. Chem. 2004;14:61.
- [6] Masuda Y, Nagahama D, Itahara H, Tani T, Seo WS, Koumoto K. J. Mater. Chem. 2003;13:1094.
- [7] Nan J, Wu J, Deng Y, Nan C-W. Solid State Commun. 2002;124:243.
- [8] Zhang FP, Lu QM, Zhang JX. J. Alloys Compd. 2009;484:550.
- [9] Patterson AL. Phys Rev 1939;56:978.
- [10] Kato M, Goto Y, Umehara K, Hirota K, Yoshimura K. Physica B 2006;378-380:1062.
- [11] Mercurio D, Champarnaud-Mesjard JC, Frit B, Conflant P, Boivin JC, Vogt T. J. Solid State Chem. 1994;112:1.
- [12] Koshibae W, Tsutsui K, Maekawa S. Phys. Rev. B 2000;62:6869.
- [13] Maignan A, Pelloquin D, Hebert S, Klein Y, Hervieu M. Bol. Soc. Esp. Ceram. V. 2006;45:122.

1  
2  
3  
4 **Figure captions**  
5  
6  
7  
8

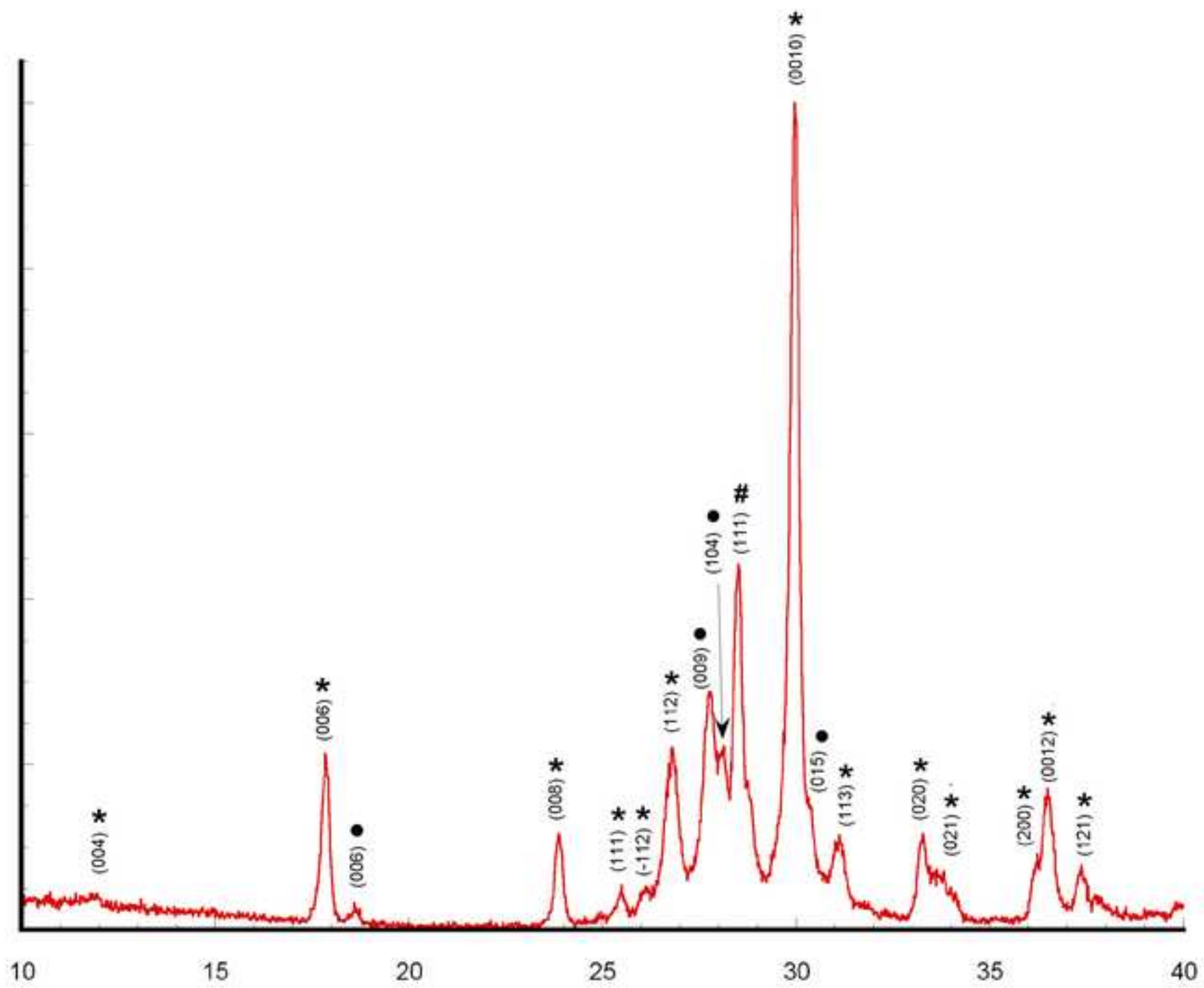
9 **Fig. 1.** XRD plot of the  $\text{Bi}_2\text{Sr}_2\text{Co}_{1.8}\text{O}_x$  samples. Peaks are marked with a \* for the  
10 thermoelectric  $\text{Bi}_2\text{Sr}_2\text{Co}_{1.8}\text{O}_x$  phase, •  $\text{Bi}_{0.75}\text{Sr}_{0.25}\text{O}_y$  non thermoelectric phase  
11  
12 ( $\bar{R}3m H'$ ), and # for Si (used as reference).  
13  
14  
15  
16  
17  
18

19 **Fig. 2.** Representative SEM micrographs of  $\text{Bi}_2\text{Sr}_2\text{Co}_{1.8}\text{O}_x$  ceramics. a) transversal  
20 fractured surface, and b) longitudinal polished surface. Different contrasts  
21  
22 correspond to  $\text{Bi}_2\text{Sr}_2\text{Co}_{1.8}\text{O}_x$  (grey), SrO (dark grey), and  $\text{Bi}_{0.75}\text{Sr}_{0.22}\text{O}_y$  (white).  
23  
24  
25  
26  
27  
28

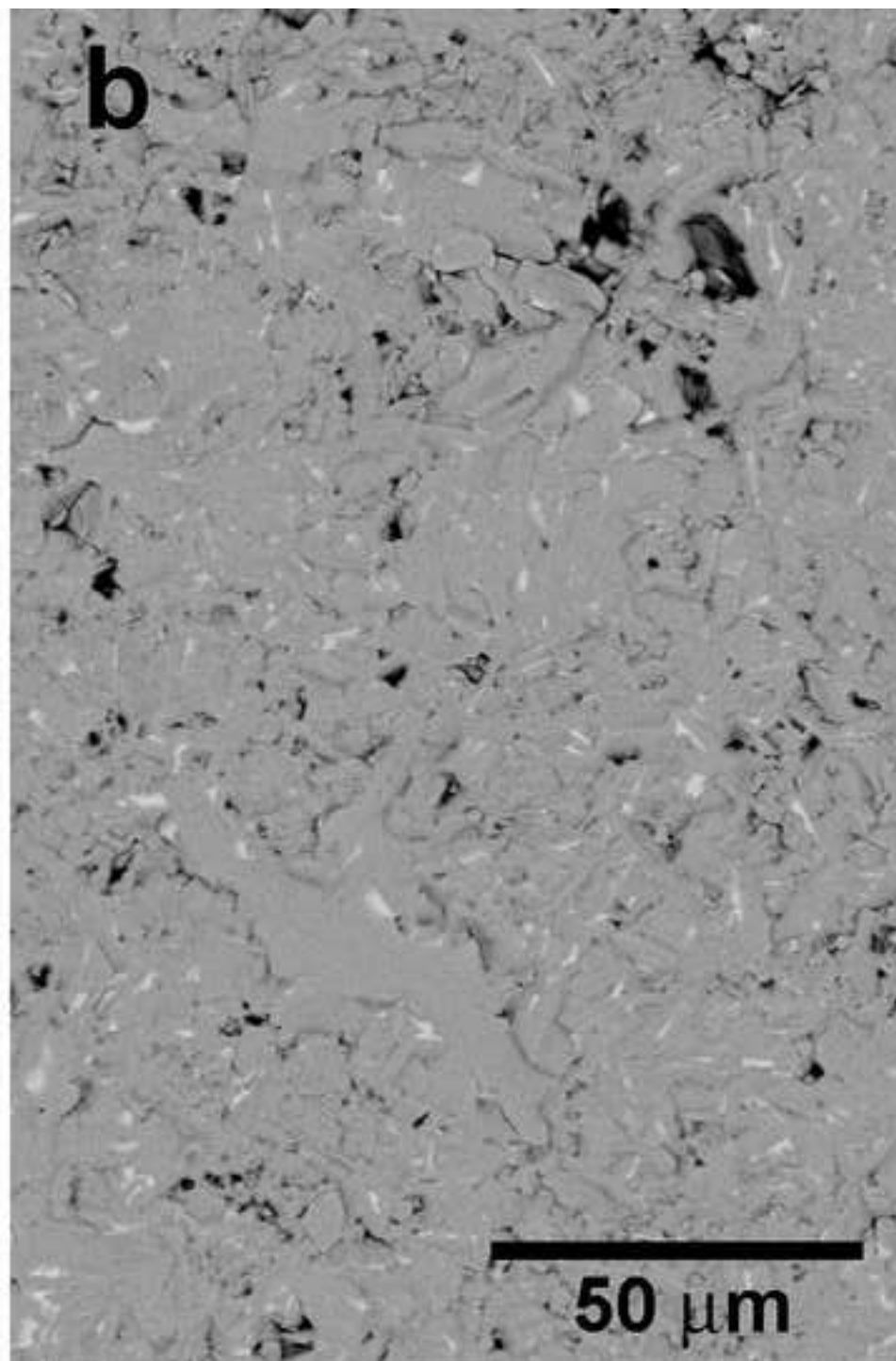
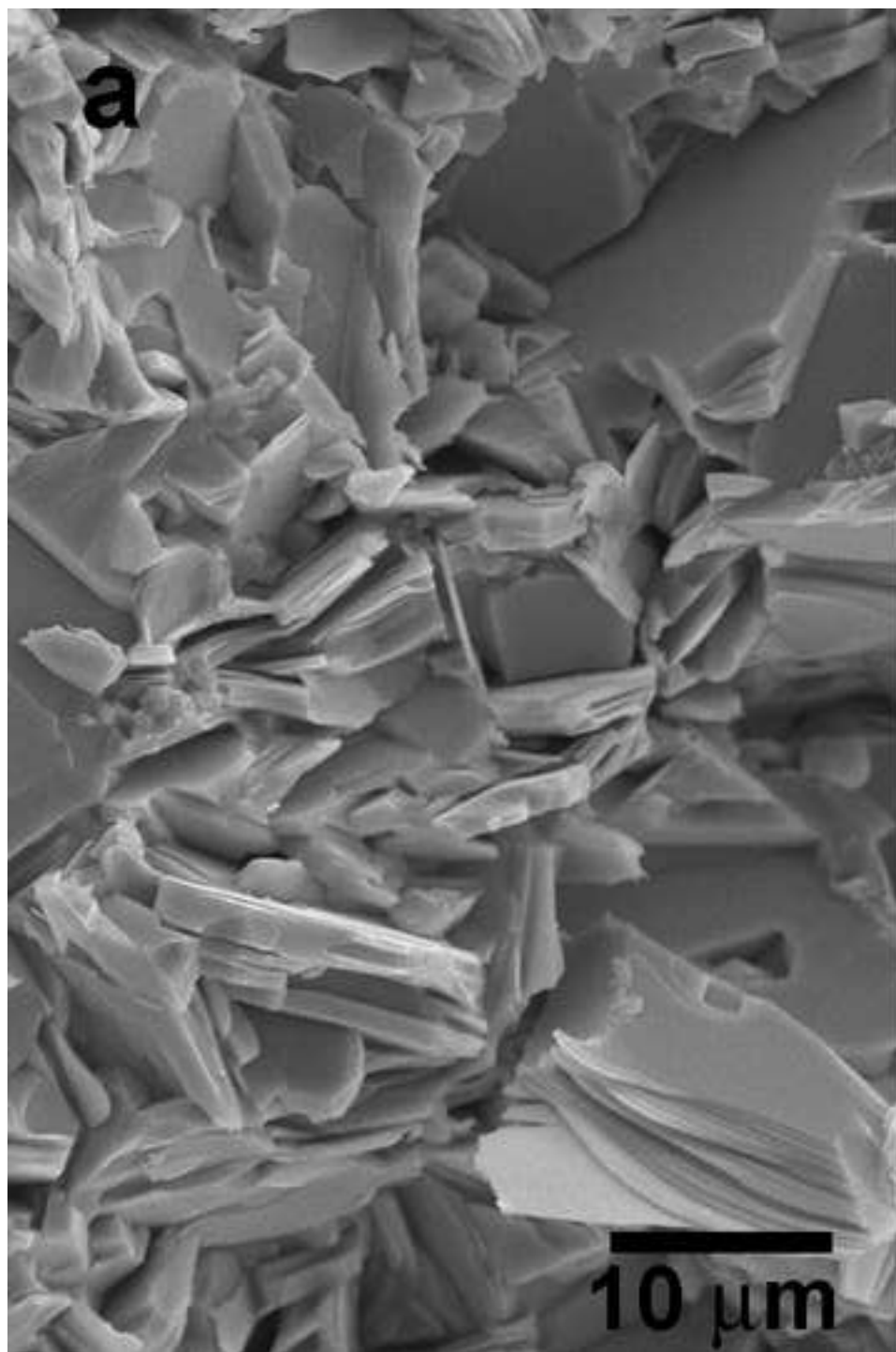
29 **Fig. 3.** Temperature dependence of  $\rho$  (•) and S (■) for polycrystalline  $\text{Bi}_2\text{Sr}_2\text{Co}_{1.8}\text{O}_x$   
30 materials.  
31  
32  
33  
34  
35

36 **Fig. 4.** Temperature dependence of PF for polycrystalline  $\text{Bi}_2\text{Sr}_2\text{Co}_{1.8}\text{O}_x$  materials.  
37  
38  
39  
40  
41  
42  
43  
44  
45  
46  
47  
48  
49  
50  
51  
52  
53  
54  
55  
56  
57  
58  
59  
60  
61  
62  
63  
64  
65

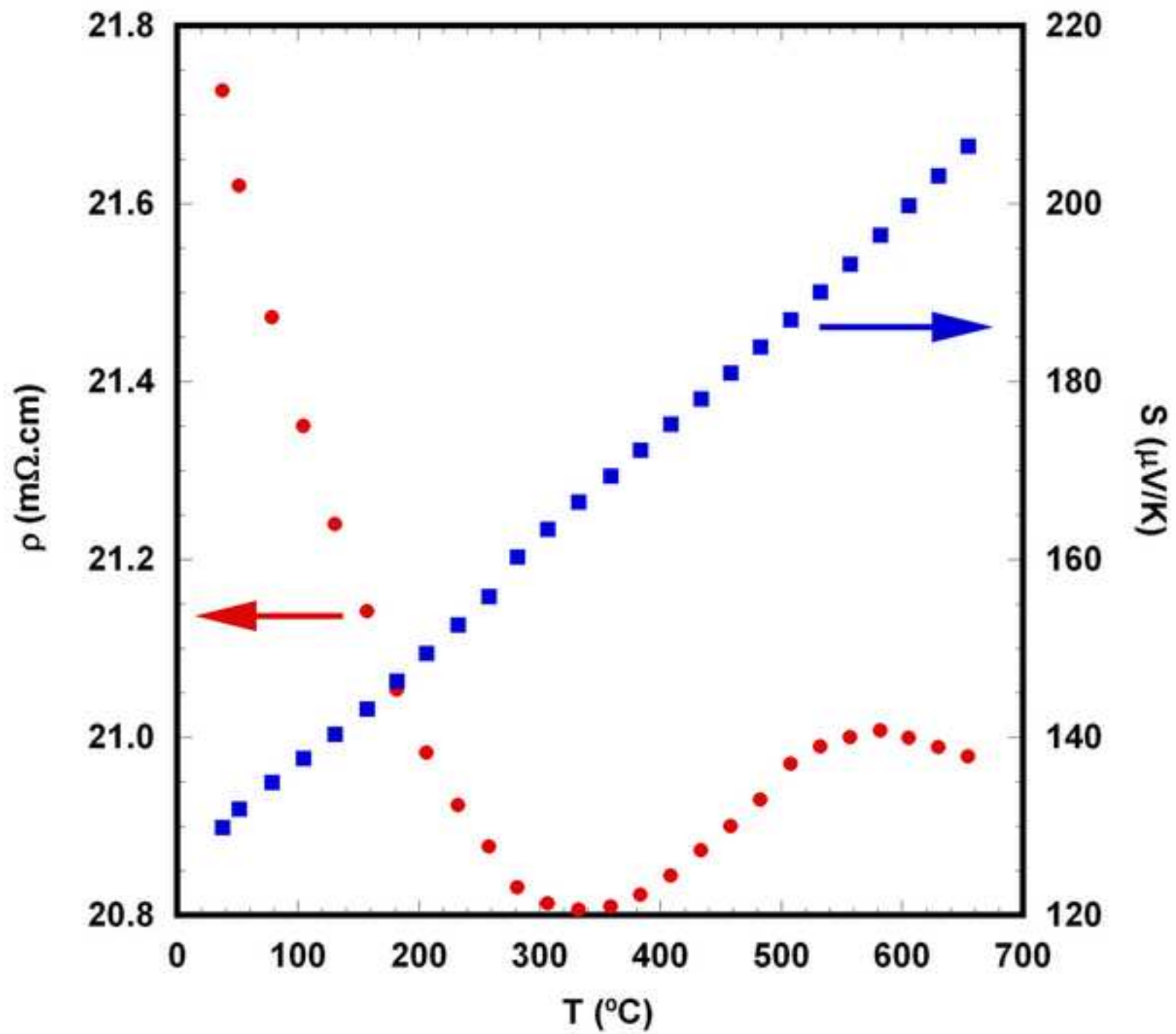
Figure(s)  
[Click here to download high resolution image](#)



Figure(s)  
[Click here to download high resolution image](#)



Figure(s)  
[Click here to download high resolution image](#)



Figure(s)

[Click here to download high resolution image](#)

